



Cite this: *Chem. Sci.*, 2025, **16**, 13564

All publication charges for this article have been paid for by the Royal Society of Chemistry

Received 28th February 2025  
Accepted 2nd July 2025

DOI: 10.1039/d5sc01624j  
[rsc.li/chemical-science](http://rsc.li/chemical-science)

## 1 Introduction

Per- and polyfluoroalkyl substances (PFAS) are a group of synthetic chemicals widely used in industrial and consumer applications since the 1940s. Their unique chemical properties, particularly their hydrophobic and lipophobic nature, have led to their extensive use in products such as non-stick cookware, water-resistant textiles, food packaging, and firefighting foams. However, their remarkable stability and resistance to environmental degradation have resulted in widespread contamination of water, soil, and air. The persistence of PFAS in the environment, combined with their bioaccumulative nature, has raised significant concerns regarding their impact on human health and ecosystems. Chronic exposure to PFAS has been linked to adverse health outcomes, including thyroid disorders, liver damage, immune suppression, developmental toxicity, and certain cancers. Among PFAS compounds, perfluorooctanoic acid (PFOA) and perfluorooctane sulfonic acid (PFOS) are the most extensively studied and are widely recognized as critical threats to environmental and public health.<sup>1–4</sup> Recent studies have identified harmful health effects associated with PFAS

precursors, such as fluorotelomer alcohols (FTOHs) and polyfluoroalkyl phosphoric acids (PAPs), which convert into perfluoroalkyl carboxylic acids (PFCAs).<sup>5</sup> Humans are exposed to these compounds through inhalation and ingestion. Indoor air and dust, particularly air conditioning filter dust,<sup>6</sup> have been identified as significant sources of PFAS exposure,<sup>7</sup> with detectable levels of PFOA, PFOS, and short-chain PFAS. Volatile organic compounds (VOCs) exacerbate this issue by increasing indoor FTOH levels. Additionally, polyfluoroalkyl phosphates in wastewater sludge contribute to FTOH formation, further elevating the risk of exposure *via* water consumption.<sup>8</sup> These findings underscore the urgent need for improved treatment methods and regulatory measures to manage emerging PFAS compounds. Regulatory agencies have responded by setting stringent limits on PFAS concentrations in drinking water, such as the recent U.S. Environmental Protection Agency (EPA) maximum contaminant levels (MCLs) of 4 parts per trillion (ppt) for PFOA and PFOS, with additional limits on other PFAS compounds.<sup>9,10</sup>

Current regulations require effectively detecting and mitigating PFAS contamination that remains a major challenge. The detection of PFAS needs high sensitivity and selectivity at trace concentrations. Traditional analytical techniques, such as liquid chromatography-tandem mass spectrometry (LC-MS/MS), are highly accurate but expensive, time-consuming, and impractical for real-time monitoring.<sup>11</sup> Alternative detection strategies, including electrochemical sensors, fluorescence-based methods, *etc.*, offer promising advantages in terms of

<sup>a</sup>Department of Building, Civil and Environmental Engineering, Concordia University, Montreal, QC, H3G 1M8, Canada. E-mail: [Jaehoon.hwang@concordia.ca](mailto:Jaehoon.hwang@concordia.ca)

<sup>b</sup>NanoScience Technology Center, Department of Chemistry, University of Central Florida, Florida, USA. E-mail: [tzhai@ucf.edu](mailto:tzhai@ucf.edu)

† Electronic supplementary information (ESI) available. See DOI: <https://doi.org/10.1039/d5sc01624j>



cost-effectiveness, portability, and real-time capabilities, yet require further improvements in detection limits and robustness.<sup>9,12</sup>

The PFAS can be removed through non-destructive and destructive approaches. Non-destructive methods include physical adsorption using activated carbon, ion exchange resins,<sup>13</sup> and filtration (e.g. microfiltration, ultrafiltration, nanofiltration and reverse osmosis).<sup>14</sup> These techniques primarily serve as separation techniques rather than complete degradation solutions, resulting in secondary waste disposal challenges. Destructive approaches include incineration, ultrasonication, plasma-based oxidation, advanced oxidation processes (AOPs), and oxidative sulfur species.<sup>4,15–17</sup> Complete PFOA mineralization has also been reported,<sup>2,18</sup> achieving 100% defluorination using oxidative species such as persulfate, hydroxyl radicals, and aprotic solvents. However, adding extra chemicals to an aquatic ecosystem cannot meet the goal of removing PFAS without introducing other chemicals. Furthermore, other parameters such as the cost of chemical transportation and storage, and complex operational processes will increase the treatment cost.<sup>1</sup> In addition, traditional PFAS removal operation relies on periodic lab testing to assess contamination levels. A combined system with real-time monitoring allows for immediate adjustments, optimizing the removal process and preventing breakthrough contamination. Continuous monitoring ensures that removal technologies only operate when needed. It prevents overuse or underuse of treatment materials in the PFAS removal process, extending the lifespan of the removal system and reducing waste.

Recognizing these challenges, recent efforts have focused on integrating PFAS detection and remediation into multifunctional platforms capable of both monitoring and removal/degradation.<sup>19–21</sup> Electrochemically active materials, conjugated polymers, metal-organic frameworks (MOFs), and nanomaterial-based hybrid systems have emerged as potential candidates for achieving simultaneous PFAS detection and removal. These integrated approaches not only enhance the PFAS detection and removal efficiency but also reduce resource consumption and enable real-time monitoring, providing a more effective strategy for PFAS management. However, several limitations, including mass transfer constraints at ultra-trace concentrations, material stability, and long-term performance, must be addressed to transform these technologies from laboratory-scale research to practical applications. Furthermore, artificial intelligence (AI) and machine learning (ML) are playing an increasingly vital role in PFAS monitoring, recognition, classification, and remediation.<sup>22–33</sup> AI-driven models have been employed for predictive analytics, optimizing treatment conditions, and enhancing sensor performance. By leveraging real-time data from detection systems, AI can dynamically adjust remediation processes, improving efficiency and reducing operational costs. Despite these advancements, the full integration of AI into PFAS detection-remediation frameworks remains largely unexplored and represents a promising avenue for future research.

This perspective critically examines the current landscape of PFAS detection and remediation technologies, highlighting

recent advancements in integrated solutions. It evaluates the challenges associated with conventional and emerging approaches, discusses the role of nanomaterials and electrochemical and optical-based strategies, and explores the potential of AI-driven tools in PFAS management. By addressing the key scientific and technological gaps, this work aims to provide insights into the development of more effective, scalable, and sustainable strategies for tackling PFAS contamination in water systems.

## 2 Current PFAS management technology trends

### 2.1 PFAS removal technologies

As previously discussed, selecting an appropriate treatment method depends on factors such as the specific PFAS compounds present, their concentrations, the characteristics of the contaminated medium, and economic considerations. Among existing PFAS removal technologies, electrochemical treatment offers several advantages. First, it operates using only electricity and electrodes, reducing the need for added chemicals. Its byproducts—harmless salts, gases, and degraded organic matter—minimize secondary waste production. Second, electrochemical oxidation can completely degrade PFAS to non-detectable levels under optimized conditions. Unlike some other methods, it is effective against both short-chain and long-chain PFAS. Third, electrochemical systems can be designed as compact, modular units, making them ideal for on-site treatment at industrial sites, wastewater facilities, and contaminated groundwater locations. This reduces the need for transporting contaminated water or disposing of spent treatment media. Fourth, electrochemical detection and removal can be integrated into a single system, enabling real-time monitoring and remediation for more efficient PFAS management. Therefore, the discussion of PFAS removal technologies focuses on electrochemical degradation.

Electrochemical degradation of PFAS involves both oxidation and hydrolysis and has the potential to achieve complete degradation to HF and CO<sub>2</sub> free of external chemicals. For PFOA, the degradation mechanism comprises the following steps:

(i) Initially, direct electrooxidation and Kolbe decarboxylation of the carboxylate group (COO<sup>−</sup>) generate C<sub>7</sub>F<sub>15</sub><sup>·</sup> radicals.<sup>3,34</sup>

(ii) Subsequently, as reported in the literature, these radicals can react with O<sub>2</sub>,<sup>4,35</sup> H<sub>2</sub>O,<sup>36</sup> or OH<sup>·</sup> radicals (see ESI†), leading to stepwise cleavage of the C<sub>n</sub>F<sub>2n</sub><sup>·</sup> molecular chain. This reaction produces CF<sub>2</sub> units (released as CO<sub>2</sub> and HF) and shorter C<sub>n−1</sub>F<sub>2n−2</sub><sup>·</sup> chains. The degradation proceeds *via* repeated cycles until complete mineralization of the original PFAS molecule is achieved. However, the degradation rate and degree of mineralization depend on the recalcitrance of the intermediate by-products. Thus, shorter-chain degradation products may inhibit the catalytic reaction by increasing the activation energy required, thereby reducing removal efficiency over time.



The progress of the electrochemical removal of PFAS has been nicely reviewed.<sup>37–40</sup> The electrochemical degradation mechanism of PFAS suggests that PFAS can be removed completely. As a matter of fact, an early study by Gomez-Ruiz and coworkers achieved the successful removal of up to 99.7% of PFAS using boron-doped diamond electrodes.<sup>41</sup> It is important to note that efficient generation of radicals is necessary for the effort. The electro-Fenton process, which applies electrical potential in an electrochemical cell to generate oxidative species such as  $\text{H}_2\text{O}_2$ , is considered a viable option. Conventional AOPs are less effective for PFAS degradation due to the negligible reactivity of  $\text{OH}^-$  radicals<sup>42</sup> and the absence of hydrogen in PFAS. However, electrochemical processes can oxidize PFAS on the anode, generating radicals like  $\text{C}_n\text{F}_{2n+1}^\cdot$ , while *in situ* hydrogen peroxide production enhances the degradation rate through hydroxyl radical formation. For instance, Liu and coworkers reported a 90% mineralization of PFOA at an initial concentration of 50 ppm using an electro-Fenton system with  $\text{H}_2\text{O}_2$  electro-generated *in situ* on hierarchically porous carbon.<sup>43</sup> These advanced electrochemical methods provide a promising pathway for overcoming the challenges of PFAS degradation, offering efficient, scalable solutions that minimize reliance on external chemicals while effectively addressing the persistence of PFAS in environmental water sources.

## 2.2 PFAS detection techniques

The detection of PFAS, even at trace levels, is essential due to the significant health risk posed by even minimal exposure.<sup>39</sup> To address this concern, regulatory agencies such as the U.S. Environmental Protection Agency (EPA) have implemented stringent maximum contaminant levels (MCLs) for certain PFAS compounds in drinking water. These MCLs, such as 4 parts per trillion (ppt) for PFOA and PFOS, and 10 ppt for perfluorononanoic acid (PFNA), perfluorohexane sulfonate (PFHxS), and hexafluoropropylene oxide dimer acid (HFPO-DA, commonly known as GenX Chemicals), require highly sensitive analytical techniques capable of detecting PFAS at ultra-trace levels.<sup>9,10,39</sup> Low PFAS concentration results in limited mass transfer to electrodes in electrochemical detection methods. To mitigate this issue, a pre-adsorption step can be beneficial when operating in the ppt range.

Chromatographic techniques coupled with mass spectrometry (e.g., GC-MS, LC-MS, and HPLC-MS/MS) have remained the benchmark for PFAS analysis due to their high sensitivity and accuracy. The EPA-approved Method 537.1 utilizes solid-phase extraction (SPE) followed by liquid chromatography-tandem mass spectrometry (LC-MS/MS). This approach enables detection at concentrations as low as 0.71–2.8 ppt which aligns with current regulatory thresholds. However, while LC-MS/MS is highly effective, it requires expensive equipment, trained personnel, and lengthy sample preparation steps, making it less suitable for routine, large-scale monitoring, or rapid field assessments.<sup>9,12,44</sup> Consequently, alternative detection strategies have emerged, including techniques based on optical and electrochemical principles. These methods offer advantages such as versatility, high sensitivity, portability, simplicity, cost-

effectiveness, and real-time monitoring capabilities, making them promising tools for rapid PFAS detection.<sup>9,12</sup>

Optical detection methods, including fluorescence (“turn-on” or “turn-off”), colorimetric techniques, surface-enhanced Raman scattering (SERS), resonance light scattering, and surface plasmon resonance approach, have gained significant attention because of high sensitivity, simplicity, and suitability for on-site and real-time monitoring.<sup>9,12</sup> Although these methods show promise for rapid screening, further development is necessary to lower their detection limits and expand their applicability to different PFAS molecules. Many optical techniques currently have difficulties in reaching the stringent detection limits required for environmental and regulatory purposes, such as the EPA's health advisory levels for drinking water. Moreover, improvement is needed to enhance the selectivity to differentiate ppt-level PFAS from other interfering substances with similar functional groups. Therefore, further advancement in detection sensitivity, specificity, and applicability to various PFAS species is essential.<sup>9,12</sup> Innovations in nanomaterials, molecular imprinting, and signal integration across optical modalities offer pathways to meet the requirement. For instance, some optical methods have achieved the detection limit of sub-ppb levels.<sup>45–52</sup> A molecularly imprinted polymer incorporated with carbon quantum dots (QDs) achieved the detection limit of 65 parts per quadrillion (ppq) for PFOS detection.<sup>45</sup> In addition, lanthanide-doped nanocrystals combined with covalent organic frameworks attained an impressive PFOS detection limit of 75 ppq.<sup>46</sup> Other approaches, such as colorimetric and fluorescence bioassays using gold nanoparticles (AuNPs) and QDs, have reached detection limits as low as 5, and 2.5 ppt.<sup>47,48</sup> Genetically engineered bacterial biosensors have also been explored, achieving 10 ppt detection limits for PFOS and PFOA.<sup>49</sup> SERS-based sensors,<sup>50</sup> fiber optic biosensors,<sup>51</sup> and MIP-based optical fiber sensors<sup>52</sup> have also shown high sensitivity, detecting PFAS at sub-ppb levels. Furthermore, Chen *et al.*<sup>53</sup> and Harrison and Waters<sup>54</sup> have reported optical platforms capable of detecting and discriminating multiple PFAS molecules, demonstrating advanced selectivity and multiplexing capabilities.

Electrochemical sensors are increasingly recognized as robust, cost-effective, highly sensitive, and portable solutions for PFAS detection. These sensors rely on electron transfer at the electrode–solution interface, generating an electrical signal that can be measured and used for analyte quantification through techniques such as voltammetry, amperometry, potentiometry, impedimetry, electrochemiluminescence (ECL), and photochemical-based sensing.<sup>9,12,55</sup> However, the electrochemical inertness of PFAS presents a significant challenge that requires the development of advanced strategies to enhance detection performance.<sup>9,56</sup> To address this challenge, modified electrodes, and redox mediators have been employed, achieving detection limits as low as sub-ppb levels in many cases.<sup>44,56–65</sup> Beyond optical and electrochemical sensors, other techniques such as high-performance liquid chromatography (HPLC) combined with optical or electrochemical systems have shown strong potential for PFAS analysis.<sup>66</sup> Furthermore, innovative non-conventional approaches, such as flow rate analysis,<sup>67</sup> and



Table 1 AI applications in PFAS management

Application	AI-based techniques	Key results/performance	Ref.
Source identification (AFFF vs. non-AFFF)	<i>k</i> -Nearest neighbors algorithm ( <i>k</i> NN), support vector machines (SVM), RF, deep neural network (DNN)	Best performance with DNNs (accuracy = 96.3%)	22
Detection and characterization	Principal component analysis (PCA), <i>t</i> -distributed stochastic neighbor embedding ( <i>t</i> -SNE)	Distinguishing the Raman spectra of 40 different PFAS compounds	23
Prediction of GenX contamination risk in private wells by integrating data on land use, proximity to PFAS sources, and weather patterns	Bayesian networks	High accuracy (AUC = 0.85)	24
Prediction of four different short-chain PFAS occurrence in groundwater using data of potential PFAS sources, soil and hydrogeologic characteristics, and land use	Bayesian networks	High predictive accuracy with AUC > 0.96	25
Prediction of private wells at risk of PFAS contamination by integrating data on PFAS sources, geology, hydrology, and soil properties	RF classifier	Area under the receiver operating characteristics curve (AUROC) scores = 0.74 to 0.86	26
Prediction of PFAS concentration in wells by integrating co-contaminant fingerprints, hydrological and soil properties, and proximity to contamination sources	Linear and RF regressors	RF achieved spearman correlation of 0.64 and accuracy of 91% (AUC = 0.90)	27
Classification	DNN	High accuracy	28
Liquid chromatography retention time prediction for over 2000 PFAS	No-code ML (orange) with multi-linear regression, SVM	High internal validation ( $R^2 > 0.98$ , MAE < 6.5 s); external robustness ( $R^2 > 0.80$ , MAE ~40 s)	29
Prediction of PFAS bioactivity	RF, DNN	Best performance with DNN (average area under the curve (AUC) = 0.916)	30
C–F bond dissociation energy prediction and chemical trends categorization	RF, DNN, <i>t</i> -SNE	Best performance with DNN ( $R^2 = 0.93$ )	31
Prediction of PFAS removal via adsorption	XGBoost	High accuracy	32
Prediction of PFAS removal in constructed wetlands	DNN	High accuracy (MAE = 27.27)	33

thermal detection using molecular imprinting,<sup>68</sup> have also achieved detection limits as low as the sub-ppb range.

A comparative evaluation of current PFAS detection technologies reveals critical trade-offs among sensitivity, practicality, and applicability. Chromatographic methods, particularly LC-MS/MS, remain the regulatory benchmark due to their exceptional sensitivity and specificity at ultra-trace levels. However, these techniques require expensive instrumentation, highly trained personnel, and involve labor-intensive procedures, limiting their suitability for rapid or in-field monitoring. In contrast, optical sensing technologies offer advantages including portability, cost-efficiency, and potential for real-time detection, though challenges persist in achieving parts-per-trillion detection limits and sufficient selectivity within complex environmental matrices. Electrochemical sensors provide a promising compromise between sensitivity and affordability and are well-suited for miniaturized, field-deployable platforms; nonetheless, the inherent electrochemical inertness of PFAS necessitates advanced

surface modification strategies to enhance sensor performance. Biosensors, incorporating molecularly imprinted polymers or engineered biological elements, demonstrate improved selectivity but may face stability issues under variable environmental conditions. The choice of an appropriate detection method depends on specific requirements such as detection limit, operational context (laboratory vs. field), infrastructure availability, and the balance among accuracy, cost, and operational complexity.

### 2.3 AI applications for PFAS monitoring and management

AI and ML have emerged as transformative tools in PFAS management, detection enhancement, predictive modeling, and remediation strategies. Table 1 summarizes key AI-driven approaches relevant to PFAS research.

In detection and source identification, ML-based classification models have been employed to differentiate between PFAS contamination sources, achieving over 96% accuracy in distinguishing aqueous film-forming foam (AFFF) and non-AFFF



origins.<sup>22</sup> Chemometric techniques combined with Raman spectroscopy have enabled the classification of PFAS structures based on molecular fingerprints, aiding non-targeted analysis.<sup>23</sup> Bayesian networks have been used to predict the contamination risks and occurrence mapping of GenX,<sup>24</sup> and four different short-chain PFASs.<sup>25</sup> Random forest (RF) models have also predicted PFAS concentrations and contamination risks in wells with high accuracy by integrating environmental and contamination source data.<sup>26,27</sup> Additionally, tools such as PFAS-Atlas have been developed for PFAS classification and visualization of chemical space, streamlining structure–property analyses.<sup>28</sup> AI models have also optimized liquid chromatography retention time predictions, minimizing the need for extensive experimental calibration in PFAS quantification.<sup>29</sup> Furthermore, AI has shown promise in predictive modeling to assess PFAS behavior and transformation,<sup>30,31</sup> and in PFAS removal optimization. ML techniques, including extreme gradient boosting (XGBoost), have identified key factors influencing adsorption efficiency,<sup>32</sup> while artificial neural networks (ANNs) have improved PFAS removal predictions in constructed wetlands compared to traditional isotherm models.<sup>33</sup> Beyond conventional supervised ML methods, recent advances in transfer learning and semi-supervised learning have shown strong potential for PFAS modeling under data-scarce conditions. For instance, a transfer learning framework employing graph attention networks (GATs) and a weighted loss function significantly improved the identification of persistent, bio-accumulative, mobile, and toxic (PBMT) chemicals, including PFAS, even with limited and imbalanced datasets.<sup>69</sup> In addition, a semi-supervised metric learning approach was developed to predict PFAS bioactivity across multiple biological targets, achieving high classification accuracy and offering interpretable structure–activity relationships.<sup>70</sup> These next-generation AI models enhance the robustness and generalizability of predictions for environmental occurrence and toxicological effects. As integrated detection–remediation frameworks evolve, the incorporation of such advanced AI approaches with real-time

monitoring and treatment data will be crucial for developing adaptive and responsive PFAS control systems.

### 3 Advanced PFAS technologies for integrated detection–remediation systems (current approaches, challenges and gaps)

Integrated approaches for PFAS detection and remediation are still in the early stages, with limited research exploring multi-functional platforms that combine fluorescence, adsorption, and electrochemical methods. Although these preliminary studies show promise for simultaneous detection and treatment, further advancements in material design, system integration, and scalability are essential to overcome existing limitations and enable practical applications. This section overviews significant advancements, addresses challenges, and highlights innovative materials and hybrid strategies that can pave the way for more effective PFAS management.

#### 3.1 Detection and removal of PFOA and PFOS using a two-in-one platform

A novel multifunctional system (Fig. 1) has been developed to address the simultaneous detection and removal of PFOA and PFOS from water. Chen and co-workers have incorporated a detection module utilizing a signal-amplified conjugated polymer (PF-DBT-Im) donor–acceptor architecture to enable hypersensitive and selective ratiometric fluorescence monitoring.<sup>19</sup> Through aggregation-induced Förster resonance energy transfer (FRET), PF-DBT-Im exhibits a distinct blue-to-magenta emission color change upon interaction with PFOA or PFOS under UV light. This mechanism facilitated a precise detection with limits of 6.12 nM for PFOA and 14.3 nM for PFOS, overcoming challenges like environmental interference and emission fluctuation errors. A smartphone-integrated portable device further facilitated real-time, on-site

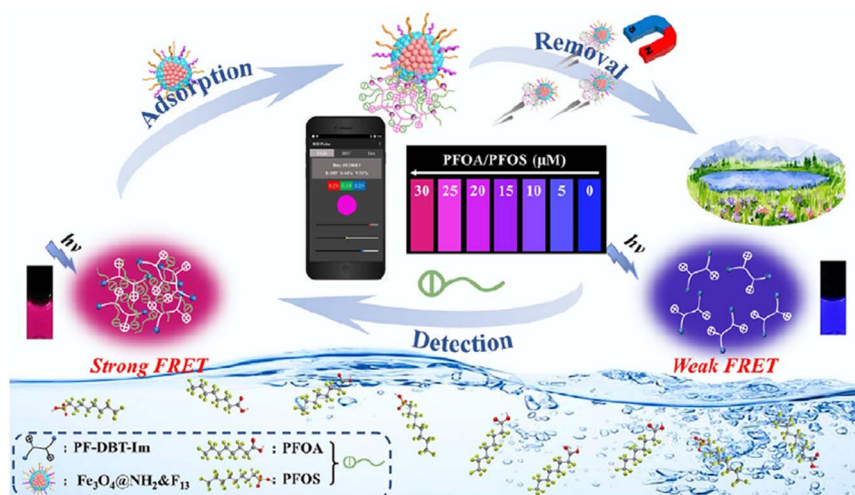


Fig. 1 Schematic illustration of the two-in-one platform for PFOA/PFOS detection and removal.<sup>19</sup>



monitoring, leveraging a simple UV-light chamber and mobile application for capturing and analyzing emission changes.

For the removal process, surface-functionalized magnetic nanoparticles ( $\text{Fe}_3\text{O}_4@\text{NH}_2\&\text{F}_{13}$ ) served as smart adsorbents. Functionalized with amino groups and perfluorinated *n*-octyl chains, these nanoparticles exhibited strong electrostatic and hydrophobic interactions with PFAS molecules, enabling selective adsorption and rapid magnetic separation. Removal efficiencies of 95.68% for PFOA and 96.99% for PFOS were achieved, with the design preventing secondary pollution and enabling effective pollutant capture using an external magnet. These removal efficiencies were obtained using authentic environmental water samples, including tap water, pool water, and river water from the Weihe River (Xi'an, Shaanxi, China). The samples underwent pretreatment to reduce matrix interferences, involving heating and the addition of  $\text{Ba}^{2+}$  and  $\text{Cl}^-$  ions to remove organic solvents and surfactants such as sodium dodecyl sulfate (SDS) and sodium dodecyl benzene sulfonate (SDBS). Subsequently, the pretreated samples were spiked with known concentrations of PFOA and PFOS to assess the system's

performance under controlled contamination conditions.<sup>19</sup> Additionally, the dual functionality of PF-DBT-Im supported real-time monitoring of the adsorption process.

This integrated system represents a significant advancement in PFAS management by combining ultra-sensitive detection with efficient remediation. However, the reliance on adsorption necessitates further treatment of separated PFAS or spent adsorbents to achieve complete degradation. Future advancements could enhance detection sensitivity to sub-ppb levels and integrate degradation mechanisms, creating a more comprehensive and sustainable solution for PFAS contamination.

### 3.2 Detection and degradation of PFOA with a bi-functional electrode

A novel approach has been introduced for the simultaneous detection and degradation of PFOA in water, utilizing a bi-functional molecularly imprinted polymer (MIP)-based MOF-driven carbon nanofiber (Co/Fe@CNF) electrode. This system integrated highly sensitive electrochemical detection with

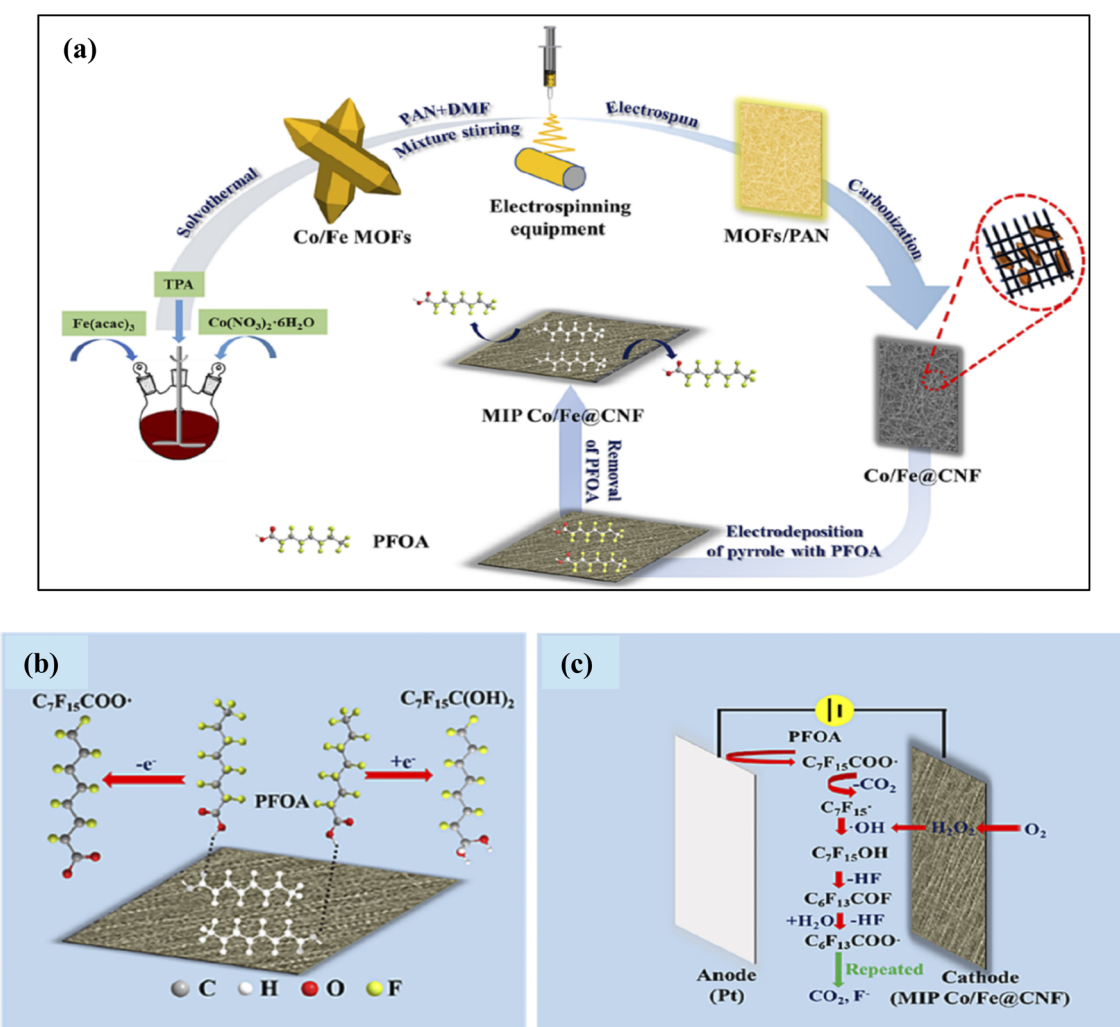


Fig. 2 (a) Schematic representation of the MIP Co/Fe@CNF fabrication process, (b) electrochemical detection mechanism of PFOA using MIP Co/Fe@CNF, (c) probable degradation pathway for PFOA using MIP Co/Fe@CNF.<sup>20</sup>



efficient electro-Fenton (EF) degradation, showcasing a significant advancement in PFAS management.<sup>20</sup> The electrode combines Co/Fe alloy-deposited carbon nanofibers, derived from bimetallic MOF precursors, with a polypyrrole-based MIP layer.

The fabrication process (Fig. 2a) involved synthesizing Co/Fe MOFs using a solvothermal method with  $\text{Fe}(\text{acac})_3$ ,  $\text{Co}(\text{NO}_3)_2 \cdot 6\text{H}_2\text{O}$ , and terephthalic acid as precursors. These MOFs were electrospun with a polyacrylonitrile (PAN)-DMF solution and carbonized to form Co/Fe@CNF. To impart molecular recognition, an MIP layer was electropolymerized onto the nanofiber surface using pyrrole and PFOA as a template molecule, followed by template removal. This process created molecularly imprinted cavities, enabling selective recognition and adsorption of PFOA through O–H– $\pi$  hydrogen bonding.

For detection, the MIP Co/Fe@CNF electrode served as an anode in differential pulse voltammetry (DPV), achieving an impressive detection limit of  $1.073 \times 10^{-9}$  M. The detection mechanism (Fig. 2b) involved the oxidation of PFOA to  $\text{C}_7\text{F}_{15}\text{COO}^{\cdot}$  and subsequent reduction. The molecularly imprinted cavities facilitated the strong adsorption of PFOA at the electrode surface, significantly enhancing the sensitivity and selectivity.

In addition to detection, the MIP Co/Fe@CNF electrode was employed as a cathode in the EF system for PFOA degradation. The electrode catalyzed the generation of hydrogen peroxide ( $\text{H}_2\text{O}_2$ ) via the oxygen reduction reaction, which decomposed into hydroxyl radicals ( $\text{HO}^{\cdot}$ ) for effective degradation. Imprinted cavities on the electrode enhanced the adsorption of PFOA and its intermediates, reducing the distance between free radicals and target molecules and increasing degradation efficiency. Under optimal conditions, the system achieved a remarkable degradation efficiency of 93% within 180 minutes (Fig. 2c),

along with an 86.3% reduction in total organic carbon (TOC) and a 67.5% defluorination rate, indicating substantial mineralization.

This integrated approach demonstrates excellent stability, reusability, high sensitivity, and effective degradation, providing a promising solution for PFOA management. However, challenges remain in broadening the platform's applicability to other PFAS compounds, addressing pH dependence, achieving complete mineralization, and simplifying the fabrication process for large-scale implementation. Future developments could focus on overcoming these limitations, enabling a more versatile and scalable technology for real-world applications.

### 3.3 Detection and real-time monitoring of photocatalytic degradation of PFOA using a ratiometric fluorescent probe

An innovative approach for detecting PFOA and monitoring its photocatalytic degradation in real-time was proposed using lanthanide-based MOFs (Ln-MOFs) as ratiometric fluorescent probes.<sup>21</sup> Fluorescence sensing methods have proven effective for PFOA detection, as discussed in Section 2.2. However, the novelty of this research lies in the development of a fluorescent probe that can detect both PFOA (reactants) and fluoride ions ( $\text{F}^-$ , products), enabling real-time monitoring of the catalytic reaction.

MOF-76 ( $\text{Tb} : \text{Eu} = 29 : 1$ ) was identified as the optimal ratiometric fluorescent probe due to its distinct fluorescence properties, which allowed the discrimination between PFOA and fluoride ions. The probe was synthesized *via* a solvothermal method (Fig. 3a), using a specific molar ratio of  $\text{Tb}^{3+}$  and  $\text{Eu}^{3+}$  to precisely tune its fluorescence characteristics. The synthesis process involved dissolving  $\text{TbCl}_3 \cdot 6\text{H}_2\text{O}$  and  $\text{EuCl}_3 \cdot 6\text{H}_2\text{O}$  in a mixture of DMF, ethanol, and water, followed by heating in

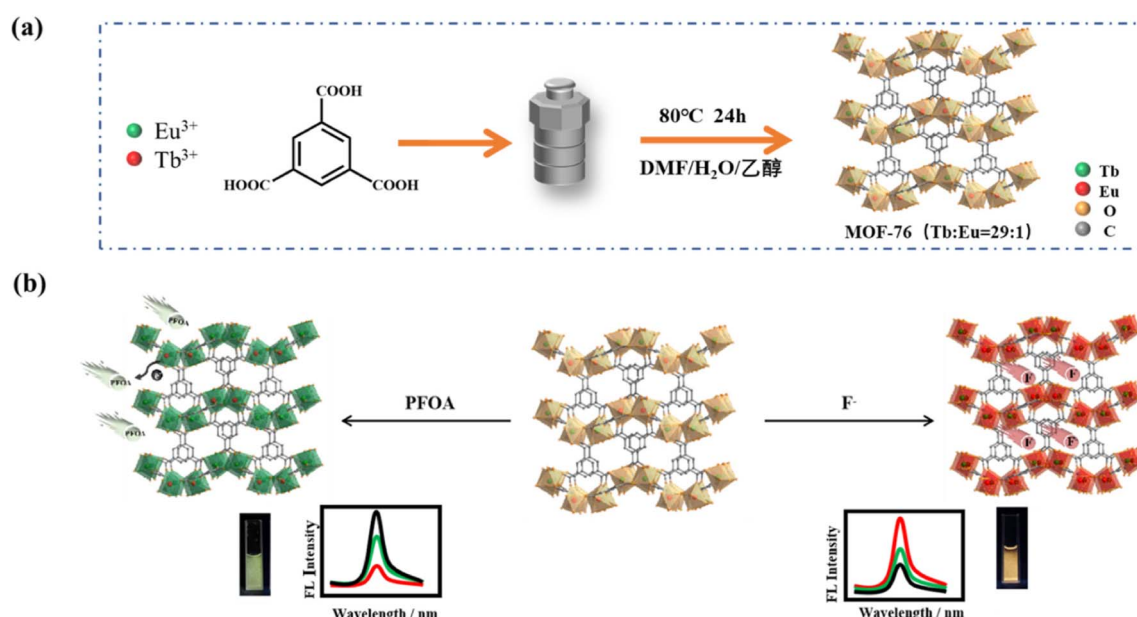


Fig. 3 The conceptual framework for (a) the synthesis of MOF-76 ( $\text{Tb} : \text{Eu} = 29 : 1$ ) and (b) the ratiometric fluorescence-based monitoring of PFOA degradation during photocatalysis.<sup>21</sup>



a stainless-steel reactor at 80 °C for 24 hours. The unique fluorescence mechanism was based on photo-induced electron transfer (PET) between MOF-76 and PFOA molecules, leading to fluorescence quenching. As degradation progressed, solvent water molecules in the MOF pores were replaced by F<sup>-</sup> ions, resulting in fluorescence enhancement. The schematic in Fig. 3b illustrates the probe's functionality: PFOA quenches the red fluorescence of Eu<sup>3+</sup>, leaving the dominant green fluorescence from Tb<sup>3+</sup>. However, as F<sup>-</sup> is released during degradation, the red fluorescence was restored and enhanced, causing a visually distinguishable color transition from green to orange-red. This change directly correlated with degradation progress, and the G/R fluorescence intensity ratio allowed for quantitative tracking. A three-dimensional relationship graph of the G/R ratio, conversion rate, and time enables real-time, naked-eye visualization of PFOA degradation. This method represents a significant advancement over conventional techniques, such as LC-MS, which require extensive pre-treatment and complex instrumentation.

The photocatalytic degradation process, facilitated by Pt-TiO<sub>2</sub> under UV light irradiation, efficiently broke down PFOA into fluoride ions and short-chain perfluoroalkyl intermediates. The probe demonstrated detection limits of 0.0127 mM for PFOA and 0.00746 mM for F<sup>-</sup>, with recoveries of 99.3–102.7% (RSD = 2.2–4.4%) for PFOA and 100.7–105.3% (RSD = 3.9–6.8%) for F<sup>-</sup> in real water samples. These results highlight the probe's practical applicability for dynamic and quantitative monitoring of catalytic reactions in environmental systems.

The limitation of this system includes a relatively high detection limit, potential interferences from other anions, and the need for further optimization to extend its applicability to a broader range of PFAS compounds. Additionally, while the system enables efficient real-time tracking of PFOA degradation, it does not directly contribute to the complete mineralization or removal of PFAS. Therefore, further integration with remediation technologies, such as photocatalytic degradation or adsorption processes, is necessary to achieve comprehensive PFAS elimination.

## 4 Future directions for integrated (detection and remediation) solutions for PFAS management through data-driven approaches

PFAS contamination in environmental systems varies significantly in concentration, composition, and co-contaminants, requiring adaptable detection and treatment solutions. Nanotechnology has enabled the development of highly sensitive sensors and efficient degradation materials,<sup>71</sup> selective PFAS capture, real-time sensing, and PFAS degradation in an integrated step. However, challenges such as material recyclability, toxicity concerns, and the long-term environmental impact of nanomaterials must be thoroughly evaluated before scaling beyond laboratory conditions. Most nanomaterial-based systems lack comprehensive life cycle assessments (LCA) to evaluate their sustainability and stability.<sup>71</sup> A promising direction is the

development of multifunctional nanomaterials capable of detecting, adsorbing, and degrading PFAS while incorporating cost-effective, reusable, and environmentally sustainable materials to improve economic feasibility and long-term safety. Hybrid nanostructures, such as bimetallic catalysts (e.g., Co/Fe-based MOFs), plasmonic nanoparticles, and functionalized carbon nanotubes, can offer high surface area, selective binding sites, and catalytic activity for electrochemical oxidation and photocatalysis. Additionally, bio-based sorbents or MOFs with tunable porosity should be explored to enhance the sustainability and cost-effectiveness of detection-remediation systems.

Electrochemical methods hold great potential for enabling simultaneous PFAS detection and treatment. Electrochemically active materials, such as nanomaterials, alloys, chalcogenides, and nitrides, can be incorporated onto electrode surfaces to facilitate direct or indirect PFAS electrooxidation, correlating measured current with pollutant concentration.<sup>72–75</sup> These systems optimize resources by reducing energy consumption, chemical usage, and processing time while enabling real-time monitoring and minimizing by-products. However, key challenges remain, including achieving a detection limit in the ppt range, improving sensitivity and selectivity for specific PFAS compounds, and enhancing degradation efficiency. To address these challenges, future efforts should focus on developing advanced electrocatalytic materials with tailored surface properties and enhanced active sites.

Mass transfer limitations at ultra-trace concentrations, especially under recently established EPA MCLs, call for more effective electrochemical and optical techniques. Future research could prioritize strategies like pre-adsorption steps to enhance PFAS transport to reactive surfaces. Functionalized adsorbents, such as amine-modified magnetic nanoparticles or fluorophilic polymer membranes, can serve as pre-concentration materials to enhance PFAS accessibility to degradation sites. Moreover, surface modifications of electrode materials using oxygen vacancies, hydroxyl radicals, or co-catalysts can increase electron transfer rates and improve degradation efficiency. Hybrid treatment approaches that combine removal (e.g., adsorption) with degradative processes (e.g., electrochemical oxidation and photocatalytic processes) may also improve the performance of integrated PFAS detection-remediation systems.

Advancements in data processing technologies such as AI and machine learning are playing an increasingly vital role in optimizing PFAS detection and remediation, as discussed in Section 2.3. However, their application in integrated PFAS detection and remediation systems remains largely underexplored, representing a promising area for future research. Beyond conventional supervised learning,<sup>22,24–28,30,32,33</sup> recent developments in transfer learning and semi-supervised modeling offer enhanced generalizability and predictive power under limited labeled data conditions,<sup>69,70</sup> which are critical for addressing complex and evolving PFAS scenarios. To fully realize the potential of AI in integrated systems, future efforts should prioritize the development of feedback-driven frameworks capable of autonomously interpreting real-time sensor data, evaluating system performance, and dynamically adjusting treatment conditions. AI-enhanced sensors could also



enable continuous real-time monitoring of PFAS contamination, thereby reducing reliance on costly and time-intensive laboratory analysis. Incorporating advanced techniques such as reinforcement learning or digital twin modeling could further support intelligent process control that adapts and improves over time, optimizing performance while minimizing chemical and energy input. When paired with multifunctional nanomaterials and real-time electrochemical or optical sensing, such adaptive AI-based platforms may pave the way toward highly efficient, scalable, and responsive PFAS management systems. These innovations have the potential to deliver precise and adaptable solutions that address the complexities of PFAS contamination across diverse water systems, thereby bridging existing gaps in field deployable detection and remediation technologies and supporting more sustainable and regulation-compliant PFAS management strategies.

## 5 Conclusion

PFAS contamination is an intensifying environmental concern that necessitates the development of integrated detection and remediation solutions that are both efficient and scalable. This perspective highlights emerging technologies designed to bridge current gaps in PFAS management. Despite recent advancements, significant challenges remain, particularly in scalability, material recyclability, and regulatory compliance. Future research should prioritize the development of multifunctional nanomaterials, the optimization of AI-driven monitoring systems, and the enhancement of treatment efficiency for ultra-low PFAS concentrations. Moreover, integrating real-time sensing with adaptive remediation strategies will be crucial for advancing field deployable solutions. Addressing these challenges will pave the way for next-generation PFAS management technologies that are sustainable, cost-effective, and regulatory compliant, ultimately mitigating the persistent threat of PFAS contamination in environmental and drinking water sources.

## Data availability

No primary research results, software or code have been included and no new data were generated or analysed as part of this review.

## Author contributions

SY and MR prepare the manuscript. LZ and JHH edit and finish the manuscript.

## Conflicts of interest

There is no conflict to declare.

## Acknowledgements

This work was supported by Natural Science and Engineering Research Council of Canada (NSERC) Discovery Grants (RGPIN-2024-05486).

## References

- 1 C. V. Reddy, R. Kumar, P. Chakrabortty, B. Karmakar, S. Pottipati, A. Kundu and B.-H. Jeon, *Chem. Eng. J.*, 2024, **152272**.
- 2 B. Trang, Y. Li, X.-S. Xue, M. Ateia, K. N. Houk and W. R. Dichtel, *Science*, 2022, **377**, 839–845.
- 3 A. Román Santiago, P. Baldaguez Medina and X. Su, *Electrochim. Acta*, 2022, **403**, 139635–139650.
- 4 S. Sharma, N. P. Shetti, S. Basu, M. N. Nadagouda and T. M. Aminabhavi, *Chem. Eng. J.*, 2022, **430**, 132895.
- 5 J. C. D'Eon, P. Crozier, V. Furdui, E. Reiner, E. Laurence Libelo and S. Mabury, *Environ. Sci. Technol.*, 2009, **43**, 4589–4594.
- 6 A. Besis, E. Botsaropoulou, C. Samara, A. Katsoyiannis, L. Hanssen and S. Huber, *Ecotoxicol. Environ. Saf.*, 2019, **183**, 109559.
- 7 A. O. De Silva, C. N. Allard, C. Spencer, G. M. Webster and M. Shoeib, *Environ. Sci. Technol.*, 2012, **46**, 12575–12582.
- 8 M. Lewis, M. H. Kim, E. J. Liu, N. Wang and K.-H. Chu, *J. Hazard. Mater.*, 2016, **320**, 479–486.
- 9 D. Thompson, N. Zolfigol, Z. Xia and Y. Lei, *Sens. Actuators Rep.*, 2024, 100189.
- 10 EPA, *Final PFAS National Primary Drinking Water Regulation*, <https://www.epa.gov/sdwa/and-polyfluoroalkyl-substances-pfas>, 2024.
- 11 A. U. Rehman, M. Crimi and S. Andreeescu, *Trends Environ. Anal. Chem.*, 2023, **37**, e00198.
- 12 H. Ryu, B. Li, S. De Guise, J. McCutcheon and Y. Lei, *J. Hazard. Mater.*, 2021, **408**, 124437.
- 13 E. Gagliano, M. Sgroi, P. P. Falciglia, F. G. A. Vagliasindi and P. Roccaro, *Water Res.*, 2020, **171**, 115381.
- 14 B. C. Crone, T. F. Speth, D. G. Wahman, S. J. Smith, G. Abulikemu, E. J. Kleiner and J. G. Pressman, *Crit. Rev. Environ. Sci. Technol.*, 2019, **49**, 2359–2396.
- 15 J. N. Meegoda, B. Bezerra de Souza, M. M. Casarini and J. A. Kewalramani, *Int. J. Environ. Res. Public Health*, 2022, **19**(24), 16397.
- 16 K. H. Kucharzyk, R. Darlington, M. Benotti, R. Deeb and E. Hawley, *J. Environ. Manage.*, 2017, **204**, 757–764.
- 17 H. N. Hussain, M. I. Jilani, F. Imtiaz, T. Ahmed, M. B. Arshad, M. Mudassar and M. N. Sharif, *Green Anal. Chem.*, 2025, **12**, 100225.
- 18 N. Wang, H. Lv, Y. Zhou, L. Zhu, Y. Hu, T. Majima and H. Tang, *Environ. Sci. Technol.*, 2019, **53**, 8302–8313.
- 19 X. Chen, S. Hussain, Y. Tang, X. Chen, S. Zhang, Y. Wang, P. Zhang, R. Gao, S. Wang and Y. Hao, *Sci. Total Environ.*, 2023, **860**, 160467.
- 20 Y. Wang, R. Ren, F. Chen, L. Jing, Z. Tian, Z. Li, J. Wang and C. Hou, *Sep. Purif. Technol.*, 2023, **310**, 123257.
- 21 M. Song, R. Yu, Y. Shang, K. Tashpulatov, H. Sun and J. Zeng, *Chemosphere*, 2024, **363**, 142946.
- 22 T. C. Kibbey, R. Jabrzemski and D. M. O'Carroll, *Chemosphere*, 2020, **252**, 126593.
- 23 Y. Chen, Y. Yang, J. Cui, H. Zhang and Y. Zhao, *J. Hazard. Mater.*, 2024, **465**, 133260.
- 24 J. Roostaei, S. Colley, R. Mulhern, A. A. May and J. M. Gibson, *J. Hazard. Mater.*, 2021, **411**, 125075.



25 R. Li and J. MacDonald Gibson, *Front. Environ. Sci.*, 2022, **10**, 958784.

26 X. C. Hu, B. Ge, B. J. Ruyle, J. Sun and E. M. Sunderland, *Environ. Sci. Technol. Lett.*, 2021, **8**, 596–602.

27 S. George and A. Dixit, *J. Environ. Manage.*, 2021, **295**, 113359.

28 A. Su, Y. Cheng, C. Zhang, Y.-F. Yang, Y.-B. She and K. Rajan, *Sci. Total Environ.*, 2024, 171229.

29 Y. Fan, Y. Deng, Y. Yang, X. Deng, Q. Li, B. Xu, J. Pan, S. Liu, Y. Kong and C.-E. Chen, *Environ. Sci.:Adv.*, 2024, **3**, 198–207.

30 W. Cheng and C. A. Ng, *Environ. Sci. Technol.*, 2019, **53**, 13970–13980.

31 A. Raza, S. Bardhan, L. Xu, S. S. Yamijala, C. Lian, H. Kwon and B. M. Wong, *Environ. Sci. Technol. Lett.*, 2019, **6**, 624–629.

32 E. Karbassiyazdi, F. Fattahi, N. Yousefi, A. Tahmassebi, A. A. Taromi, J. Z. Manzari, A. H. Gandomi, A. Altaee and A. Razmjou, *Environ. Res.*, 2022, **215**, 114286.

33 P. Savvidou, G. Dotro, P. Campo, F. Coulon and T. Lyu, *Sci. Total Environ.*, 2024, **934**, 173237.

34 M.-K. Kim, T. Kim, T.-K. Kim, S.-W. Joo and K.-D. Zoh, *Sep. Purif. Technol.*, 2020, **247**, 116911.

35 K. Sivagami, P. Sharma, A. V. Karim, G. Mohanakrishna, S. Karthika, G. Divyapriya, R. Saravanathamizhan and A. N. Kumar, *Sci. Total Environ.*, 2023, **861**, 160440.

36 D. Huang, K. Wang, J. Niu, C. Chu, S. Weon, Q. Zhu, J. Lu, E. Stavitski and J. H. Kim, *Environ. Sci. Technol.*, 2020, **54**, 10954–10963.

37 J. N. Meegoda, B. Bezerra de Souza, M. M. Casarini and J. A. Kewalramani, *Int. J. Environ. Res. Public Health*, 2022, **19**, 25.

38 K. Sivagami, P. Sharma, A. V. Karim, G. Mohanakrishna, S. Karthika, G. Divyapriya, R. Saravanathamizhan and A. N. Kumar, *Sci. Total Environ.*, 2023, **861**, 160440.

39 B. T.-W. Tan, N. H. H. A. Bakar and H. L. Lee, *J. Environ. Chem. Eng.*, 2024, 114990.

40 L. Shi, C. Leng, Y. Zhou, Y. Yuan, L. Liu, F. Li and H. Wang, *Environ. Sci. Pollut. Res.*, 2024, **31**, 42593–42613.

41 B. Gomez-Ruiz, S. Gómez-Lavín, N. Diban, V. Boiteux, A. Colin, X. Dauchy and A. Urtiaga, *Chem. Eng. J.*, 2017, **322**, 196–204.

42 H. F. Schroder and R. J. Meesters, *J. Chromatogr. A*, 2005, **1082**, 110–119.

43 Y. Liu, S. Chen, X. Quan, H. Yu, H. Zhao and Y. Zhang, *Environ. Sci. Technol.*, 2015, **49**, 13528–13533.

44 J. J. C. Solís, S. Yin, M. Galicia, M. S. Ersan, P. Westerhoff and D. Villagrán, *Chem. Eng. J.*, 2024, **491**, 151821.

45 Z. Jiao, J. Li, L. Mo, J. Liang and H. Fan, *Microchim. Acta*, 2018, **185**, 1–9.

46 J. Li, C. Zhang, M. Yin, Z. Zhang, Y. Chen, Q. Deng and S. Wang, *ACS Omega*, 2019, **4**, 15947–15955.

47 W. Xia, Y.-J. Wan, X. Wang, Y.-y. Li, W.-J. Yang, C.-X. Wang and S.-q. Xu, *J. Hazard. Mater.*, 2011, **192**, 1148–1154.

48 J. Zhang, Y. Wan, Y. Li, Q. Zhang, S. Xu, H. Zhu and B. Shu, *Environ. Pollut.*, 2011, **159**, 1348–1353.

49 G. Sunantha and N. Vasudevan, *Sci. Total Environ.*, 2021, **759**, 143544.

50 C. McDonnell, F. M. Albarghouthi, R. Selhorst, N. Kelley-Loughnane, A. D. Franklin and R. Rao, *ACS Omega*, 2022, **8**, 1597–1605.

51 G. Moro, F. Chiavaioli, S. Liberi, P. Zubiate, I. Del Villar, A. Angelini, K. De Wael, F. Baldini, L. M. Moretto and A. Giannetti, *Results Opt.*, 2021, **5**, 100123.

52 R. Pitruzzella, F. Arcadio, C. Perri, D. Del Prete, G. Porto, L. Zeni and N. Cennamo, *Chemosensors*, 2023, **11**, 211.

53 B. Chen, Z. Yang, X. Qu, S. Zheng, D. Yin and H. Fu, *ACS Appl. Mater. Interfaces*, 2021, **13**, 47706–47716.

54 E. E. Harrison and M. L. Waters, *Chem. Sci.*, 2023, **14**, 928–936.

55 K. Kukralova, E. Miliutina, O. Guselnikova, V. Burtsev, T. Hrbek, V. Svorcik and O. Lyutakov, *Chemosphere*, 2024, **364**, 143149.

56 R. B. Clark and J. E. Dick, *ACS Sens.*, 2020, **5**, 3591–3598.

57 M. B. Garada, B. Kabagambe, Y. Kim and S. Amemiya, *Anal. Chem.*, 2014, **86**, 11230–11237.

58 R. Ranaweera, C. Ghafari and L. Luo, *Anal. Chem.*, 2019, **91**, 7744–7748.

59 N. Karimian, A. M. Stortini, L. M. Moretto, C. Costantino, S. Bogianni and P. Ugo, *ACS Sens.*, 2018, **3**, 1291–1298.

60 Y. H. Cheng, D. Barpaga, J. A. Soltis, V. Shutthanandan, R. Kargupta, K. S. Han, B. P. McGrail, R. K. Motkuri, S. Basuray and S. Chatterjee, *ACS Appl. Mater. Interfaces*, 2020, **12**, 10503–10514.

61 P. Gogoi, Y. Yao and Y. C. Li, *ChemElectroChem*, 2023, **10**, e202201006.

62 D. Lu, D. Z. Zhu, H. Gan, Z. Yao, J. Luo, S. Yu and P. Kurup, *Sens. Actuators, B*, 2022, **352**, 131055.

63 Y. Wei, H. Liu, S. Wang, K. Yu and L. Wang, *Analyst*, 2023, **148**, 3851–3859.

64 H. B. Lamichhane and D. W. Arrigan, *Sens. Diagn.*, 2023, **2**, 938–947.

65 R. Khan, D. Andreescu, M. H. Hassan, J. Ye and S. Andreescu, *Angew. Chem.*, 2022, **134**, e202209164.

66 E. Poboży, E. Król, L. Wójcik, M. Wachowicz and M. Trojanowicz, *Microchim. Acta*, 2011, **172**, 409–417.

67 L. E. Breshears, S. Mata-Robles, Y. Tang, J. C. Baker, K. A. Reynolds and J.-Y. Yoon, *J. Hazard. Mater.*, 2023, **446**, 130699.

68 F. A. Tabar, J. W. Lowdon, M. Caldara, T. J. Cleij, P. Wagner, H. Diliën, K. Eersels and B. van Grinsven, *Environ. Technol. Innovation*, 2023, **29**, 103021.

69 H. Wang, W. Liu, J. Chen and S. Ji, *Environ. Sci. Technol.*, 2024, **59**, 578–590.

70 H. Kwon, Z. A. Ali and B. M. Wong, *Environ. Sci. Technol. Lett.*, 2022, **10**, 1017–1022.

71 M. Yadav, F. J. Osonga and O. A. Sadik, *Sci. Total Environ.*, 2024, **912**, 169279.

72 R. Ramachandran, T.-W. Chen, S.-M. Chen, T. Baskar, R. Kannan, P. Elumalai, P. Raja, T. Jeyapragasam, K. Dinakaran and G. p. Gnana kumar, *Inorg. Chem. Front.*, 2019, **6**, 3418–3439.

73 J. Baranwal, B. Barse, G. Gatto, G. Broncova and A. Kumar, *Chemosensors*, 2022, **10**, 363.

74 S. Wu and Y. H. Hu, *Chem. Eng. J.*, 2021, **409**, 127739.

75 M. Zhang, Q. Shi, X. Song, H. Wang and Z. Bian, *Environ. Sci. Pollut. Res. Int.*, 2019, **26**, 10457–10486.

